山西大学学报(自然科学版)47(3):614－623,2024
Journal of Shanxi University(Nat. Sci. Ed.)

DOI:10.13451/j.sxu.ns.2023149

铜-碳点复合物的制备及其抗菌活性研究

郭丽霞[1],刘嘉欢[1],周亮[2],马颖钰[2],张雪云[2],刁海鹏[2],刘文[2*]
(1.山西医科大学 药学院,山西 太原 030001;
2.山西医科大学 基础医学院,山西 太原 030001)

摘　要:铜绿假单胞菌(*P. aeruginosa*)是医院感染的主要病原体且耐药性强,故迫切需要开发新策略和发展高效药物分子来应对这个困境。本工作以柠檬酸和(2-甲基-5-硝基苯基)胍硝酸盐为原料,通过水热法合成了具有高效抗菌活性的蓝色荧光碳点(CDs)。通过对CDs形貌、组分以及光学性能表征,显示CDs是粒径约3 nm且分散均一的纳米球,表面含有羧基和氨基等官能团,且在光刺激下可以产生活性氧。为了增强其抗菌活性,CDs进一步与Cu^{2+}螯合得到复合物CDs@Cu。当浓度为30 μg/mL,在氙灯照射下相对于CDs对*P. aeruginosa* 85.4%的杀伤率,CDs@Cu的杀伤效率可达到99.9%。因此,该复合纳米粒子不仅可作为一种新型高效抗菌材料,而且对开发基于碳点的抗菌剂提供新思路和新方法。

关键词:铜绿假单胞菌;活性氧;铜离子;胍基
中图分类号:O614.4　　**文献标志码**:A　　**文章编号**:0253-2395(2024)03-0614-10

Preparation of Copper-Carbon Dots Complex and Its Antibacterial Activity

GUO Lixia[1], LIU Jiahuan[1], ZHOU Liang[2], MA Yingyu[2], ZHANG Xueyun[2], DIAO Haipeng[2], LIU Wen[2*]
(1. *School of Pharmacy, Shanxi Medical University, Taiyuan* 030001*, China;*
2. *School of Basic Medical Science, Shanxi Medical University, Taiyuan* 030001*, China*)

Abstract: *Pseudomonas aeruginosa* (*P. aeruginosa*) is a major pathogen of hospital-acquired infections and has high drug resistance, so it is urgent to develop new strategies and efficient drug molecules to deal with this problem. In this paper, blue fluorescent carbon dots (CDs) with high antibacterial activity was synthesized by hydrothermal method using citric acid and (2-methyl-5-nitrophenyl) guanidine nitrate as raw materials. The morphology of CDs shows that they are the uniformly dispersed nanospheres with a particle size of about 3 nm. The composition and optical properties show that there are functional groups such as carboxyl and amino groups on the surface of CDs, and the CDs can generate reactive oxygen species under light stimulation. In order to improve antibacterial activity and the ability to promote wound healing, the CDs further chelated Cu^{2+} to obtain composite CDs@Cu. The killing rate of CDs on *P. aeruginosa* under xenon lamp irradiation is 85.4% when the concentration was 30 μg/mL, and the killing efficiency of CDs@Cu can reach to 99.9%. Therefore, the composite nanoparticles can not only be used as a new and efficient antibacterial material, but also provided new ideas and methods for the development of antibacterial agents based on carbon dots.

Key words: *Pseudomonas aeruginosa*; reactive oxygen species; copper ion; guanidine group

收稿日期:2023-05-19;**接受日期**:2023-09-14
基金项目:国家自然科学基金(82071969);山西省自然科学基金(201901D111191;20210302124341);太原市迎泽区科技项目(2022)
作者简介:郭丽霞(1990-),女,山西吕梁人,博士,讲师,研究方向为纳米材料及生物应用。E-mail:guolxia@sxmu.edu.cn
* **通信作者**:刘文(LIU Wen),E-mail:liuwen@sxmu.edu.cn
引文格式:郭丽霞,刘嘉欢,周亮,等.铜-碳点复合物的制备及其抗菌活性研究[J].山西大学学报(自然科学版),2024,47(3):614-623. DOI:10.13451/j.sxu.ns.2023149

0 Introduction

Bacterial infections delay wound healing and impose a significant social and economic burden on patients and health care systems[1]. With the increase in bacterial resistance to antibiotics, infectious diseases caused by drug-resistant bacteria have become the second leading cause of death worldwide[2]. It is estimated that 700 000 people worldwide die each year from drug-resistant bacterial infections, and the cumulative total will reach 300 million by 2 050 if current trends continue[3-5]. Among these infections, gram-negative bacteria with a lipopolysaccharide protective outer membrane can restrict access to certain antibiotics and cause more serious infections[6-7]. The World Health Organization has listed some of the most serious pathogens that are highly resistant to antibiotics, and *P. aeruginosa* is one of the leading members. *P. aeruginosa* is a major pathogen of nosocomial infections, which is prone to drug resistance and is associated with pneumonia, urinary tract infections and surgical wound infections[8]. Therefore, there is an urgent need to develop novel strategies or drugs to treat *P. aeruginosa* infections.

A variety of nanomaterials, including noble metal nanoparticles, polymeric nanoparticles and carbon-based nanomaterials have been found to be used against bacterial infections[9-10]. Carbon dots (CDs), as carbon-based fluorescent nanomaterials with ultra-tiny sizes below 10 nm, excellent photoluminescence properties, low toxicity properties and tunability of surface functions. These characteristics have made CDs received much attention in the fields of bioimaging, gene/drug delivery, luminescent devices, catalysts and antibacterial drugs [11-16]. In addition, CDs containing an abundance of heteroatoms can provide active sites for their functionalized modifications through coordination and electrostatic interactions[17-18]. Antimicrobial materials based on CDs have been rapidly developed with various antimicrobial mechanisms such as DNA binding, inhibition of bacterial metabolism, photoactivation to generate reactive oxygen species (ROS) and thermal[19-20]. Guanidine groups are common functional groups in many biologically relevant molecules and are the preferred functional groups for antimicrobial drug design and development. This is because guanidinium groups are protonated at physiological pH, which facilitates interaction with anionic phospholipids within the bacterial membrane, disrupting the cell membrane and leading to lethal leakage of the cytoplasmic matrix[21-24]. Modified guanidine group in CDs will help to improve the antibacterial activity of CDs. The antibacterial activity of copper has been recognized in ancient times and its ions and complexes have been shown to have broad-spectrum antimicrobial activity[25]. Copper ions (Cu^{2+}) can penetrate bacterial cell membranes, inhibit cellular respiration and degrade DNA, thereby causing irreversible damage to bacteria. In addition, it can also promoting angiogenesis and accelerate wound healing by stabilizing the expression of hypoxia-inducible factor and the secretion of vascular endothelial growth factor[26-29]. However, most CDs currently reported have poor antimicrobial properties and are rarely able to chelate Cu^{2+}. Therefore, we speculate whether the combination of CDs and Cu ions with their respective advantages has better antibacterial activity.

Based on this, CDs with antibacterial activity were synthesized by hydrothermal method using citric acid (CA) and (2-methyl-5-nitrophenyl)guanidine nitrate as raw materials and ultrapure water as solvent. CDs can produce ROS under light stimulation. The composite material CDs@Cu was obtained by the coordination between CDs and Cu^{2+}. Compared with CDs, the CDs@Cu at the same concentration showed stronger antibacterial properties against *P. aeruginosa* and could kill 99.9% of the bacteria. This nanocomposite will provide a new strategy for the development of novel antibacterial drugs.

1 Materials and methods

1.1 Instruments and reagents

The morphology and structural characterization

of CDs were observed by Tecnai G2 20-S-TWIN field emission transmission electron microscope (TEM, FEI, USA), Multimode 8 atomic force microscope (AFM, Bruker, USA), ALPHAll FT-IR spectrometer (FT-IR, Bruker, USA), ESCALAB 250Xi X-ray photoelectron spectrometer (XPS, Thermo Scientific, USA) and D8 Advance X-ray diffractometer (XRD, Bruker, USA), respectively. The absorption and emission spectra were recorded by UH5300 UV-Vis spectrophotometer (UV-Vis, Hitachi, Japan) and F-7100 fluorescence spectrophotometer (Hitachi, Japan), respectively. The absorbance value was tested on ELx808 Enzyme Labeler (BioTeK, USA). The potential was tested on Zetasizer Nano ZS-90 Laser Particle Sizer (Malvern PANalytical, UK).

Citric acid, (2-methyl-5-nitrophenyl)guanidine nitrate, dimethyl sulfoxide (DMSO), ethanol, $CuCl_2 \cdot 2H_2O$ and 2′,7′-dichlorodihydrofluorescein diacetate (DCFH-DA) were purchased from Aladdin, Shanghai. *Pseudomonas aeruginosa*, fetal bovine serum, trypsin, thiazole blue (MTT), dulbecco's modified eagle medium (DMEM) culture medium and paraformaldehyde were purchased from Solarbio, Beijing. Luria-Bertani (LB) broth powder and nutrient agar were purchased from Shenggong Biological Engineering Co., LTD.

1.2 Preparation and characterization of CDs

Suitable amounts of CA and (2-methyl-5-nitrophenyl)guanidine nitrate were dissolved by redistilled water, and then transferred to an autoclave after complete dissolution and heated to react. During the synthesis process, the conditions were optimized. The mass ratios of (2-methyl-5-nitrophenyl)guanidine nitrate and CA were 1∶1, 1∶2 and 1∶3, respectively. The synthesis times were 4 h, 5 h and 6 h, and the temperatures were 190 ℃, 200 ℃ and 210 ℃, respectively. The reaction products were centrifuged at 10 000 r/min for 10 min, and the supernatant was collected and filtered through 0.22 μm aqueous microporous filter. Then, it dialyzed in a dialysis bag with molecular weight of 1 000 Da for 24 h. The yellow powder CDs was obtained by freeze-drying, and the apparent morphology and elemental composition were observed by TEM, AFM, XRD and XPS. The functional groups on surfaces of CDs were studied by FT-IR.

1.3 Optical properties of CDs

CDs was dissolved with redistilled water and a master batch with a concentration of 10 mg/mL was prepared and set aside. The absorption and emission spectra of CDs (0.1 mg/mL) were tested using UV-Vis and fluorescence spectrometer with excitation slit and emission slit of 5 nm and 10 nm, respectively. The stability of CDs in different concentrations of NaCl solutions (0, 29.2, 58.4, 87.6, 116.8, 146.0 and 175.2 mg/mL), PBS buffers with different pH (4.0, 5.0, 6.0, 7.0, 8.0, 9.0 and 10.0) and different times (0, 6, 12, 18, 24 and 30 days) were tested using fluorescence spectrometry. The performance of CDs in producing ROS was tested by activated 19.5 μg/mL DCFH-DA with 0.4 mg/mL NaOH in a certain ratio.

1.4 Construction and characterization of CDs@Cu

CDs (0.1 mg/mL) were incubated with different concentrations of $CuCl_2$ solution (0, 2, 4, 6, 8, 10, 12, 14, 16, 18 and 20 μg/mL) for 5 min at room temperature in a shaker, and the changes of fluorescence spectra were recorded to evaluate their performance in chelating Cu^{2+}. The changes of zeta potential of CDs before and after Cu^{2+} chelation were measured by Laser Particle Sizer. The changes of fluorescence spectra of DCFH-DA probe was used to evaluate the performance of ROS generation of CDs before and after chelating Cu^{2+}.

1.5 Cytotoxicity assay

Human normal cervical epithelial cells (HcerEpic) were used as template cells, and the toxicity of CDs and CDs@Cu to the cells was determined by MTT method. The cells were inoculated in 96-well plates at a concentration of 1×10^4 cells per well and incubated for 24 h. The culture medium was discarded and 100 μL of medium containing different concentrations of CDs and CDs@Cu was added to each well, and then incubated for 24 h.

Subsequently, 100 μL MTT was added and incubated for 4 h. Finally, MTT was discarded, and 200 μL DMSO was added, and the absorption value at 490 nm was detected by enzyme marker.

1.6 Measurement of antibacterial activity

P. aeruginosa was cultured in LB liquid medium for 9 h. The bacterial broth was centrifuged at 7 100 r/min for 2.5 min, washed twice with PBS, and the OD_{600} was 1.0. Then, 100 μL of bacterial broth was incubated with 400 μL of different concentrations of CDs (37 ℃, 15 min), and the final concentrations of CDs were 0, 10, 20, 30 and 40 μg/mL, respectively. The light group was illuminated with xenon lamp for 15 min, and light power density was 0, 25 and 50 mW/cm^2, respectively. Finally, 100 μL of bacterial solution was diluted with secondary water was spread on an agar plate. The number of colonies was counted after 18 h in the incubator, and the viability were counted.

The antibacterial performance experiment of CDs@Cu was performed as above.

1.7 SEM Characterization

The optimal antibacterial concentration of CDs@Cu was selected for SEM imaging experiments. After the antimicrobial experiment, the bacterial solution was centrifuged (10 000 r/min, 2 min), the supernatant was removed, and the obtained bacteria were resuspended in 30 μL water. Subsequently, The suspension (4 μL) was taken on a clean silicon wafer, and once the liquid was air-dried, glutaraldehyde in a volume fraction of 0.5% was added immediately was added immediately and kept overnight at 4 ℃ overnight. Finally, glutaraldehyde was removed, and eluted using a gradient of ethanol (20%, 40%, 50%, 70%, 90% and 100%). Gold was coated on the specimens to perform the SEM.

2 Results and discussion

2.1 Preparation and characterization of CDs

CA is a weak organic acid that can be used to synthesize fluorescent CDs. Guanidinium groups have better antibacterial activity. Therefore, (2-methyl-5-nitrophenyl)guanidine nitrate and CA were selected as raw materials for the synthesis of CDs with high antibacterial activity (Fig. 1(a)). The conditions for the synthesis of CDs were further optimized. The strongest fluorescence performance of carbon quantum dots was obtained at 5 h of reaction under the conditions of 1∶1 mass ratio of raw materials and 200 ℃ (Fig. 1(b)). The fluorescence performance of CDs was strongest at a mass ratio of 1∶2 between CA and (2-methyl-5-nitrophenyl)guanidine nitrate at a reaction temperature of 200 ℃ and 5 h (Fig. 1(c)). The fluorescence performance of CDs was strongest at a reaction temperature of 200 ℃ under the conditions of 5 h reaction time and 1∶2 mass ratio of raw materials (Fig. 1(d)). Therefore, the optimal reaction conditions for CDs were: mass ratio of (2-methyl-5-nitrophenyl)guanidine nitrate and CA is 1∶2, reaction time is 5 h and temperature is 200 ℃. The FT-IR results showed (Fig. 1(e)) that O—H, N—H, C—N, C—O, C=C, and C=O functional groups are present in CDs. The absorption peaks appearing at 3 430 cm^{-1} are the stretching vibrations of O—H and N—H, and 1 685 cm^{-1} are the stretching vibrations of C=C or C=O, the absorption peaks appearing at 1 385 cm^{-1} and 1 104 cm^{-1} can be the bending vibrations of C—N and C—O, respectively. The XRD results show (Fig. 1 (f)) that the broad diffraction center of CDs is 25° (2θ=25°), indicating that it's mainly composed of amorphous carbon.

The morphology of CDs was characterized by TEM and AFM (Fig. 2(a) and 2(c)), and the corresponding statistical plots are shown in Fig. 2(b) and 2(d). The results showed that the particle size and height of CDs are about 3 nm, indicating that CDs are uniformly distributed quasi-spherical nanoparticles.

The structural composition of the CDs was further characterized using XPS. As shown in Fig. 3 (a), CDs has three peaks in the full spectrum, O1s, N1s and C1s peaks at 535.1 eV, 403.8 eV and

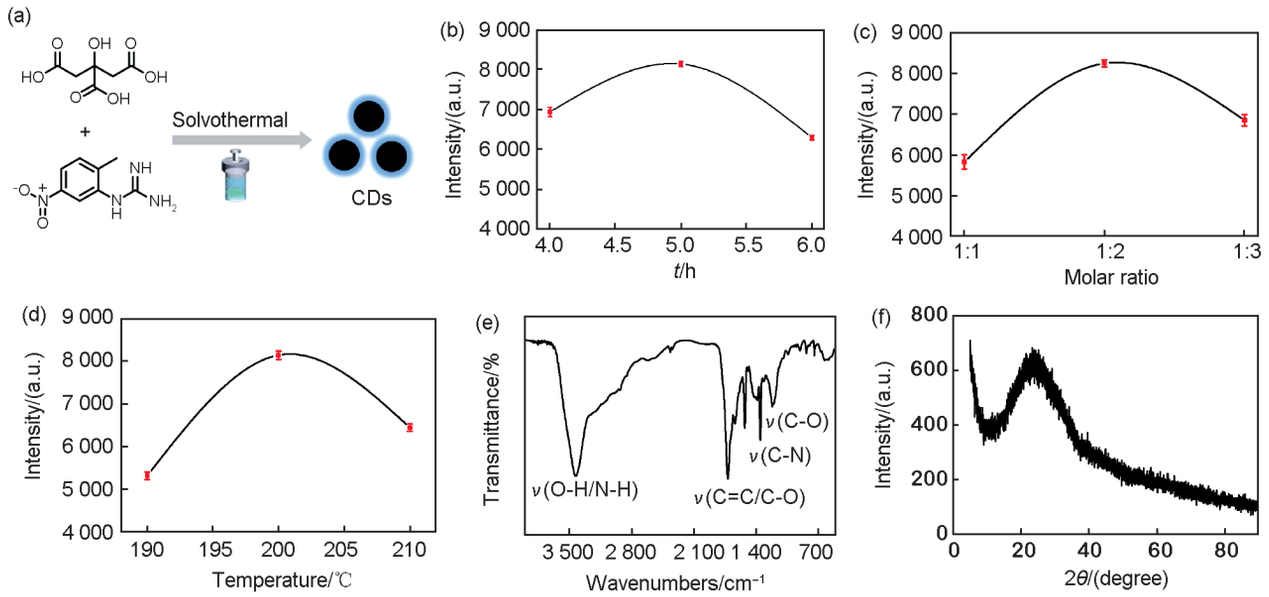

Fig. 1 Preparation and structural characterization of CDs

(a) Simple diagram of CDs preparation. The fluorescence intensity of CDs at 440 nm under (b) different reaction time, (c) different mass ratios of the reactants, and (d) different temperatures. (e) FTIR spectrum of CDs. (f) XRD pattern of CDs

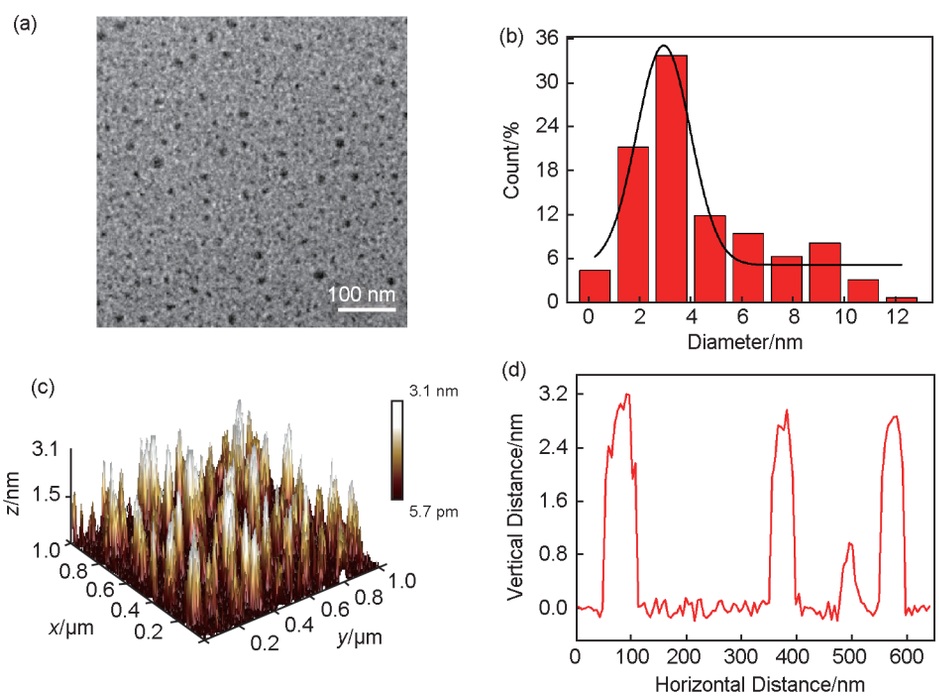

Fig. 2 Morphology characterization of CDs

(a) TEM and (b) corresponding statistical histogram of CDs. (c) AFM and (d) corresponding statistics of CDs

287.5 eV, respectively. Fig. 3(b) shows the high-resolution spectrum of O1s with two peaks of C—OH/C—O—C peak at 532.9 eV and C=O peak at 531.6 eV. The three peaks of N1s spectrum (Fig. 3(c)) are C—N—C peak at 399.7 eV, N—H peak at 400.8 eV and O=N—O peak at 406.0 eV. The four peaks of C1s spectrum (Fig. 3(d)) are C=C/C—C peak at 284.8 eV, C—N peak at 285.9 eV, C—O peak at 287.6 eV, and C=O peak at 288.9 eV. The above results of XPS show that the surface of CDs is rich in functional groups, which corresponds to the results of FT-IR.

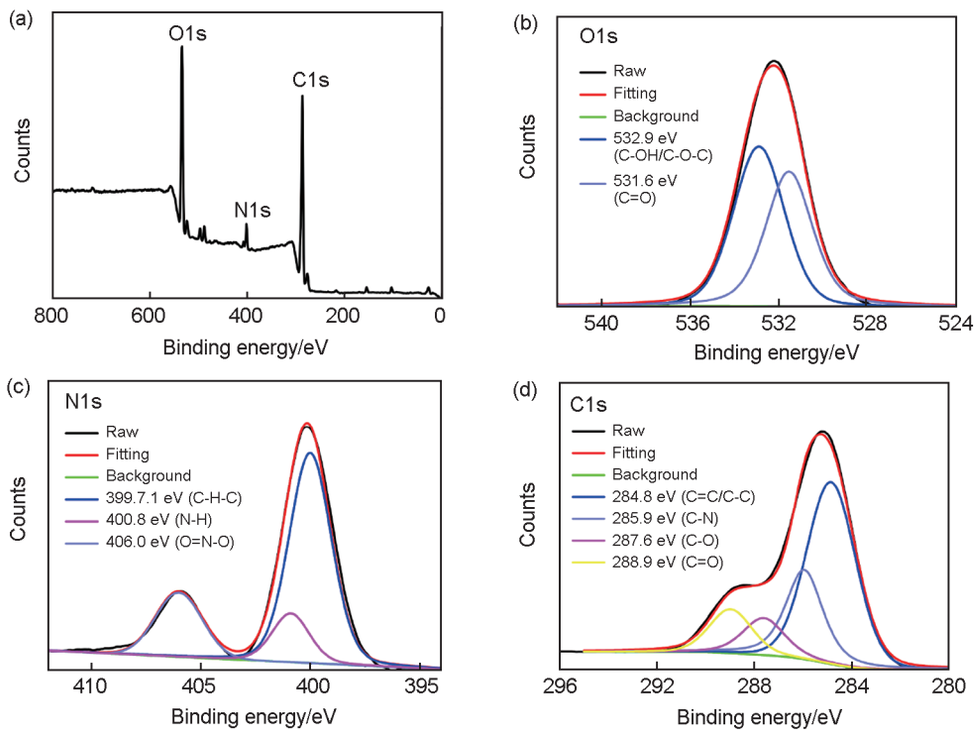

Fig. 3 XPS of CDs

(a) full spectrum; (b) O1s spectrum; (c) N1s spectrum; (d) C1s spectrum

2.2 Optical properties of CDs

After the structure of CDs was determined, the optical properties of CDs were measured. The UV-vis absorption spectra, excitation spectra and fluorescence emission spectra of CDs showed that the maximum absorption peak locates at 275 nm, the emission wavelength locates at 440 nm (Fig. 4(a)). The optimal excitation wavelength was 360 nm (Fig. 4 (b)). The stability of CDs was assessed by the change of the fluorescence intensity at 440 nm, and it was found that the fluorescence intensity was almost constant at different pH (4.0—10.0), different ionic solutions (Fig. 4(c) and 4(d)), and the fluorescence remained unaffected after 30 days (Fig. 4(e)), indicating that CDs have good stability. Finally, the performance of CDs in generating ROS under xenon lamp irradiation was examined using the commercial ROS probe DCFH-DA. The results showed in Fig. 4 (f), the fluorescence intensity of the probe is significantly enhanced by the addition of CDs, indicating that ROS could be generated.

2.3 Construction and characterization of CDs@Cu

Due to the functional groups such as amino and carboxyl groups on the surface of CDs, they can chelate metal ions to form complexes. Fig. 5(a) shows the fluorescence spectra of CDs after adding different concentrations of Cu^{2+}. It can be found that fluorescence intensity of CDs is significantly reduced, which indicates that it can effectively chelate Cu^{2+}. Fig. 5(b) shows the potential changes of CDs before and after chelating Cu^{2+}, further illustrating that CDs can chelate Cu^{2+} to form CDs@Cu. ROS generation ability of CDs@Cu and CDs were tested, and the results showed that the ability of ROS production was barely affected after chelating Cu^{2+}(Fig. 5(c)). Finally, the toxicity of CDs and CDs@Cu on HcerEpic cells was investigated, and the results showed neither was toxic to the cells (Fig. 5(d)), indicating that CDs@Cu has a good biosafety.

2.4 Antibacterial properties of CDs@Cu and CDs

Next, the killing effects of CDs on *P. aeruginosa* at different optical power densities and different concentrations were investigated. The antibacterial

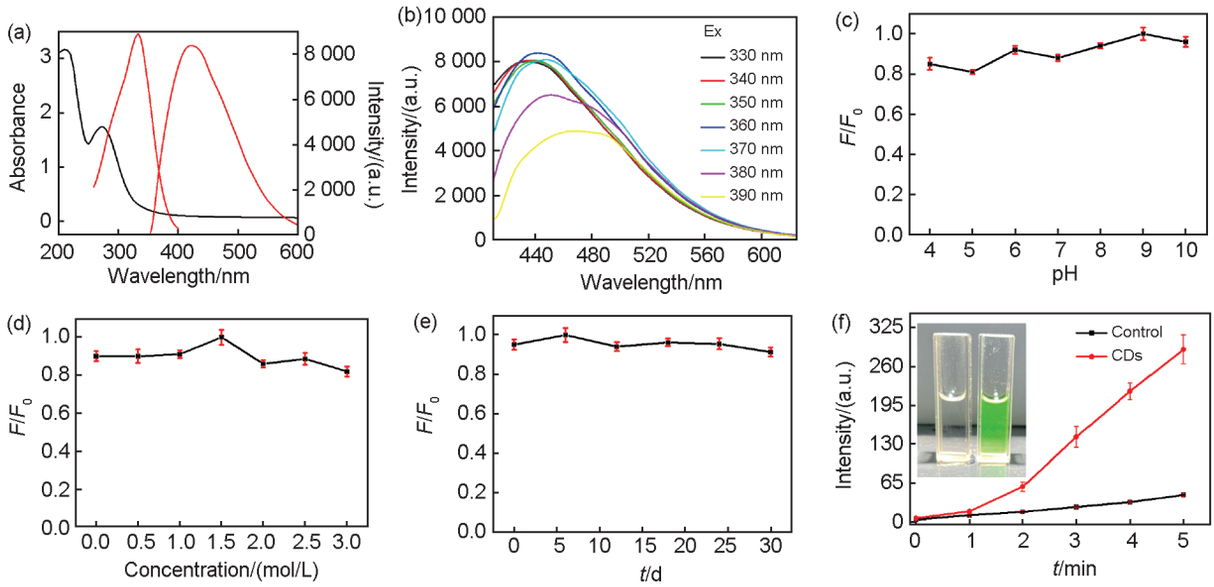

Fig. 4 Optical properties and stability of CDs

(a) UV-Vis absorption spectra, excitation spectra and fluorescence emission spectra of CDs; (b) Fluorescence emission spectra of CDs at different excitation wavelengths; Stability of CDs for (c) different pH, (d) different concentrations of NaCl, and (e) different times at room temperature; (f) Fluorescence intensities of DCFH-DA in the absence and presence of CDs upon irradiation of xenon lamp

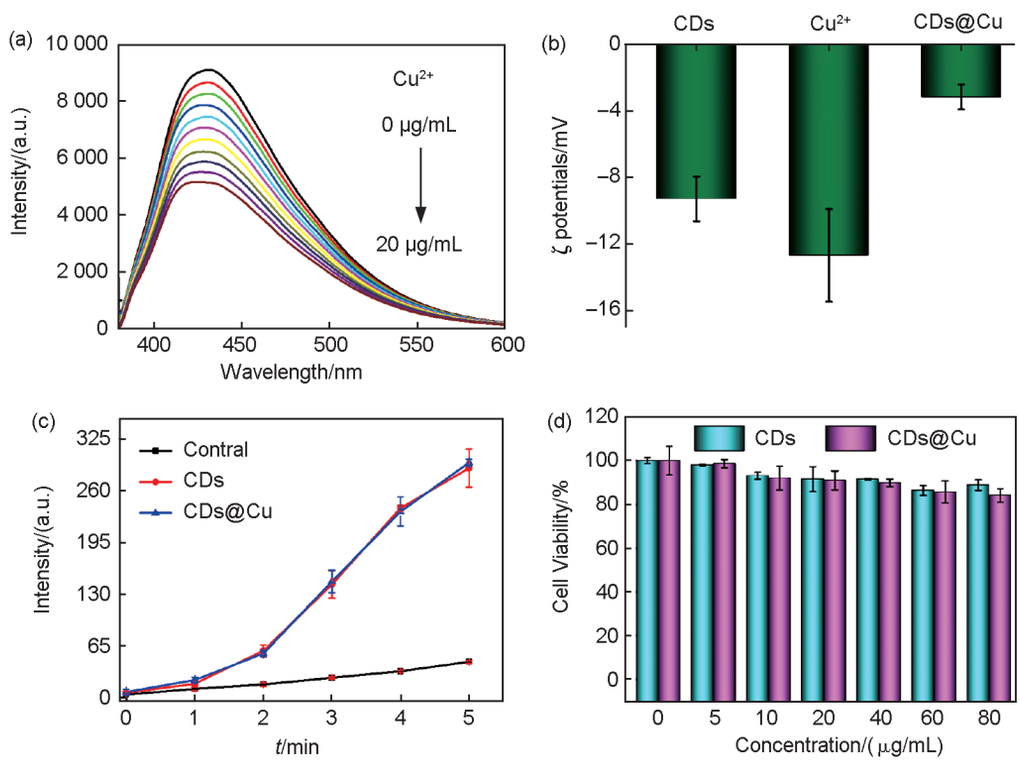

Fig. 5 Construction and characterization of CDs@Cu

(a) Fluorescence emission spectra of CDs with different concentrations of Cu^{2+}; (b) The zeta potential change of CDs before and after chelating Cu^{2+}; (c) Fluorescence intensities of DCFH-DA in the absence CDs, and presence of CDs and CDs@Cu upon irradiation of xenon lamp; (d) Cytotoxicity of different concentrations of CDs and CDs@Cu

properties of CDs gradually increased with the increase of concentration and optical power density. When CDs were irradiated at a concentration of 40 μg/mL and 50 mW/cm^2 for 15 min, there were no colonies(Fig. 6(a)) and the killing rate of *P. aeruginosa* reached 99.9% (Fig. 6(b)). These results

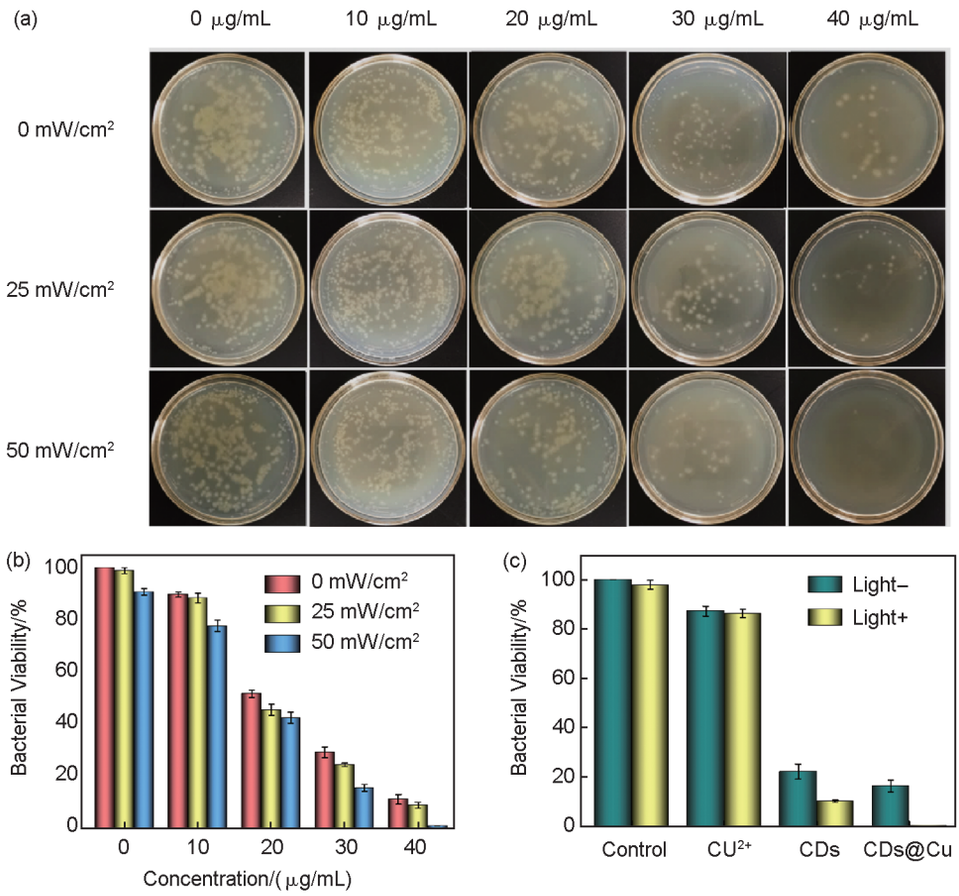

Fig. 6 Antibacterial properties of CDs before and after binding Cu^{2+}

(a) Antibacterial plate and (b) diagram of different concentrations of CDs against *P. aeruginosa* under xenon lamps with different optical power densities; (c)Antibacterial properties of CDs, Cu^{2+} and CDs@Cu at the same conditions, Cu^{2+} was 2 μg/mL, CDs and CDs@Cu was 30 μg/mL

show that CDs can kill bacteria, and ROS produced in light can further help to eliminate bacteria. Cu^{2+} has broad-spectrum antibacterial activity, which suggests that CDs chelating Cu^{2+} will enhance its antibacterial properties. When the concentration of CDs@Cu was 30 μg/mL and irradiated at 50 mW/cm² for 15 min, the killing rate of *P. aeruginosa* reached 99.9% (Fig. 6(c)). The results showed that CDs@Cu antibacterial activity is significantly higher than Cu^{2+} and CDs, which also implies that the antibacterial properties of CDs were significantly enhanced after binding Cu^{2+}.

Finally, the antibacterial properties of different concentrations of CDs@Cu were investigated. The antibacterial properties of CDs@Cu were enhanced with the increase of concentration (Fig. 7(a)), and the same results are seen in the corresponding plates (Fig. 7(b)). After clarifying its antibacterial properties, morphology of bacteria before and after treatment with CDs@Cu was characterized by SEM. It can be seen in Fig. 7(c), the morphology of bacteria collapsed after treatment with CDs@Cu.

3 Conclusion

In this work, carbon dot CDs with efficient antibacterial activity were obtained by introducing guanidine groups, which further chelated Cu^{2+} to obtain composite nanoparticles CDs@Cu with stronger antibacterial activity. CDs@Cu were found to generate ROS under light irradiation *in vitro*. The antibacterial properties were further investigated by coated plate method, and the results showed that the antibacterial properties of CDs@Cu were stronger than CDs at the same concentration. The morphology of

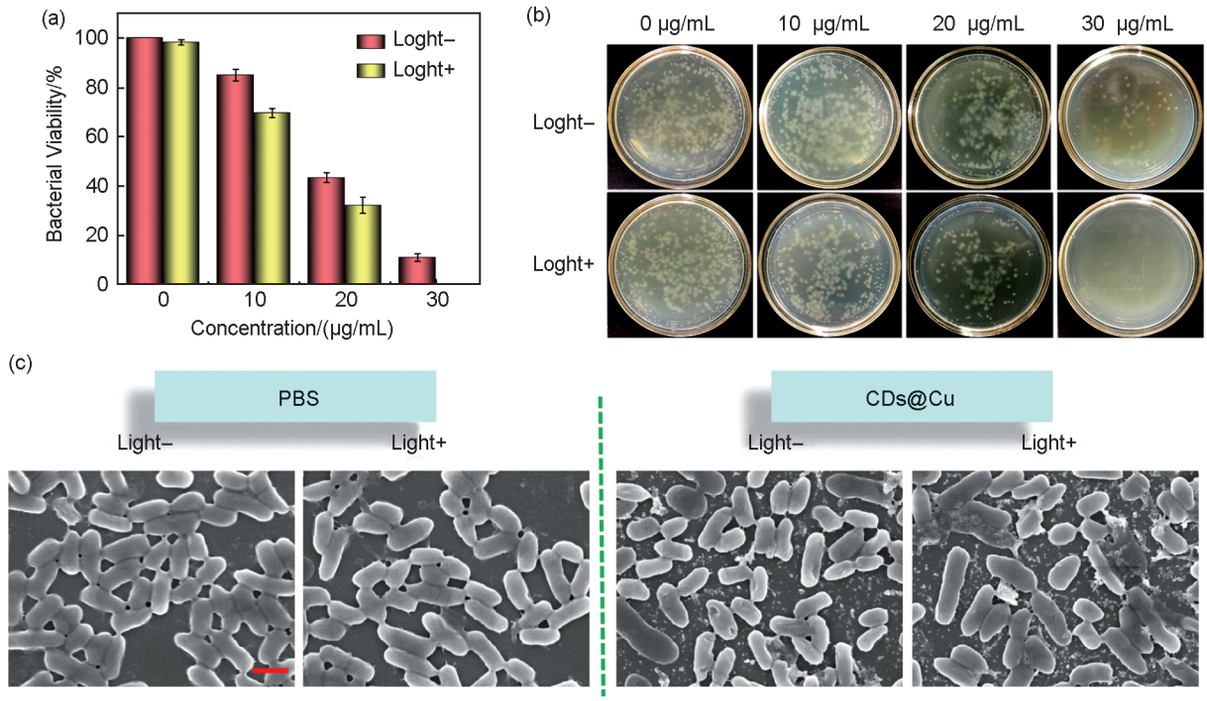

Fig. 7 Antibacterial properties of CDs@Cu

(a) Antibacterial diagram and (b) corresponding plate of different concentrations of CDs@Cu against *P. aeruginosa* upon the irradiation of xenon lamp; (c) SEM image of CDs@Cu killing bacteria, CDs@Cu was 30 μg/mL and the scale is 1 μm

P. aeruginosa underwent significant collapse after treatment with CDs@Cu. Therefore, this work will provide new ideas for the development of new efficient antibacterial materials and also provide theoretical basis for their clinical applications.

References:

[1] KUMAR V B, NATAN M, JACOBI G, *et al*. Ga@C-dots as an Antibacterial Agent for the Eradication of *Pseudomonas aeruginosa*[J]. *Int J Nanomed*, 2017, **12**: 725−730. DOI: 10.2147/ijn.s116150.

[2] CHEN F, MOAT J, MCFEELY D, *et al*. Biguanide Iridium(III) Complexes with Potent Antimicrobial Activity[J]. *J Med Chem*, 2018, **61**(16): 7330−7344. DOI: 10.1021/acs.jmedchem.8b00906.

[3] XU Q, CHANG M L, ZHANG Y, *et al*. PDA/Cu Bioactive Hydrogel with "Hot Ions Effect" for Inhibition of Drug-resistant Bacteria and Enhancement of Infectious Skin Wound Healing[J]. *ACS Appl Mater Interfaces*, 2020, **12** (28): 31255−31269. DOI: 10.1021/acsami.0c08890.

[4] WANG P Y, SONG Y Z, MEI Q, *et al*. Sliver Nanoparticles@carbon Dots for Synergistic Antibacterial Activity [J]. *Appl Surf Sci*, 2022, **600**: 154125. DOI: 10.1016/j.apsusc.2022.154125.

[5] DONG X L, LIANG W X, MEZIANI M J, *et al*. Carbon Dots as Potent Antimicrobial Agents[J]. *Theranostics*, 2020, **10**(2): 671−686. DOI: 10.7150/thno.39863.

[6] PANDEY A, DEVKOTA A, YADEGARI Z, *et al*. Antibacterial Properties of Citric Acid/B -alanine Carbon Dots Against Gram-negative Bacteria[J]. *Nanomaterials*, 2021, **11**(8): 2012. DOI: 10.3390/nano11082012.

[7] SHARMA C, SHUKLA A K, ACHARYA A. Rational Design of a FRET-based Nanoprobe of Gold-conjugated Carbon Dots for Simultaneous Monitoring and Disruption of *Pseudomonas aeruginosa* Biofilm Through Selective Detection of Virulence Factor Pyocyanin[J]. *Environ Sci : Nano*, 2021, **8**(6): 1713−1728. DOI: 10.1039/D1EN00187F.

[8] TAO Q, GUO L X, DIAO H P, *et al*. Facile Antibacterial Materials with Turbine-like Structure for *P. Aeruginosa* Infected Scald Wound Healing[J]. *Biomater Sci*, 2021, **9** (10): 3830−3837. DOI: 10.1039/d1bm00483b.

[9] OTIS G, BHATTACHARYA S, MALKA O, *et al*. Selective Labeling and Growth Inhibition of *Pseudomonas aeruginosa* by Aminoguanidine Carbon Dots[J]. *ACS Infect Dis*, 2019, **5**(2): 292−302. DOI: 10.1021/acsinfecdis.8b00270.

[10] HUANG S, SONG Y X, ZHANG J R, *et al*. Antibacterial Carbon Dots-based Composites[J]. *Small*, 2023, **19** (31): 2207385. DOI: 10.1002/smll.202207385.

[11] YANG J J, ZHANG X D, MA Y H, *et al*. Carbon Dot-based Platform for Simultaneous Bacterial Distinguishment and Antibacterial Applications[J]. *ACS Appl Mater*

Interfaces, 2016, **8**(47): 32170−32181. DOI: 10.1021/acsami.6b10398.

[12] BOOBALAN T, SETHUPATHI M, SENGOTTUVELAN N, *et al*. Mushroom-derived Carbon Dots for Toxic Metal Ion Detection and as Antibacterial and Anticancer Agents[J]. *ACS Appl Nano Mater*, 2020, **3**(6): 5910−5919. DOI: 10.1021/acsanm.0c01058.

[13] KASPRZYK W, ÅŠWIERGOSZ T, BEDNARZ S, *et al*. Luminescence Phenomena of Carbon Dots Derived from Citric Acid and Urea: A Molecular Insight[J]. *Nanoscale*, 2018, **10**(29): 13889−13894. DOI: 10.1039/C8NR03602K.

[14] WU X Y, ABBAS K, YANG Y X, *et al*. Photodynamic Anti-bacteria by Carbon Dots and Their Nanocomposites[J]. *Pharmaceuticals*, 2022, **15**(4): 487. DOI: 10.3390/ph15040487.

[15] GAO F, MA S, LI J, *et al*. Rational Design of High Quality Citric Acid-derived Carbon Dots by Selecting Efficient Chemical Structure Motifs[J]. *Carbon*, 2017, **112**: 131−141. DOI: 10.1016/j.carbon.2016.10.089.

[16] LIU Y, XU B, LU M, *et al*. Ultrasmall Fe-doped Carbon Dots Nanozymes for Photoenhanced Antibacterial Therapy and Wound Healing[J]. *Bioact Mater*, 2022, **12**: 246−256. DOI: 10.1016/j.bioactmat.2021.10.023.

[17] CHU X H, ZHANG P, LIU Y H, *et al*. A Multifunctional Carbon Dot-based Nanoplatform for Bioimaging and Quaternary Ammonium Salt/Photothermal Synergistic Antibacterial Therapy[J]. *J Mater Chem B*, 2022, **10**(15): 2865−2874. DOI: 10.1039/d1tb02717d.

[18] GAO X W, MA X T, HAN X Y, *et al*. Synthesis of Carbon Dot-ZnO-based Nanomaterials for Antibacterial Application[J]. *New J Chem*, 2021, **45**(9): 4496−4505. DOI: 10.1039/D0NJ05741J.

[19] YANG X, LI P, TANG W, *et al*. A Facile Injectable Carbon Dot/Oxidative Polysaccharide Hydrogel with Potent Self-healing and High Antibacterial Activity[J]. *Carbohydr Polym*, 2021, **251**: 117040. DOI: 10.1016/j.carbpol.2020.117040.

[20] VARGHESE M, BALACHANDRAN M. Antibacterial Efficiency of Carbon Dots Against Gram-positive and Gram-negative Bacteria: a Review[J]. *J Environ Chem Eng*, 2021, **9**(6): 106821. DOI: 10.1016/j.jece.2021.106821.

[21] KIM S H, SEMENYA D, CASTAGNOLO D. Antimicrobial Drugs Bearing Guanidine Moieties: a Review [J]. *Eur J Med Chem*, 2021, **216**: 113293. DOI: 10.1016/j.ejmech.2021.113293.

[22] PENG W, YIN H, LIU P, *et al*. Covalently Construction of Poly(hexamethylene biguanide) as High-efficiency Antibacterial Coating for Silicone Rubber[J]. *Chem Eng J*, 2021, **412**: 128707. DOI: 10.1016/j.cej.2021.128707.

[23] CHEN A, CHEN E, PALERMO E F. Guanidium-functionalized Cationic Molecular Umbrellas as Antibacterial Agents[J]. *Polym Chem*, 2021, **12**(16): 2374−2378. DOI: 10.1039/d1py00071c.

[24] SALAMA A, HASANIN M, HESEMANN P. Synthesis and Antimicrobial Properties of New Chitosan Derivatives Containing Guanidinium Groups[J]. *Carbohydr Polym*, 2020, **241**: 116363. DOI: 10.1016/j.carbpol.2020.116363.

[25] TU Y S, LI P, SUN J J, *et al*. Remarkable Antibacterial Activity of Reduced Graphene Oxide Functionalized by Copper Ions[J]. *Adv Funct Mater*, 2021, **31**(13): 2008018. DOI: 10.1002/adfm.202008018.

[26] LI J, ZHAI D, LV F, *et al*. Preparation of Copper-containing Bioactive Glass/Eggshell Membrane Nanocomposites for Improving Angiogenesis, Antibacterial Activity and Wound Healing[J]. *Acta Biomater*, 2016, **36**: 254−266. DOI: 10.1016/j.actbio.2016.03.011.

[27] ZENG J, GENG X, TANG Y, *et al*. Flexible Photothermal Biopaper Comprising Cu^{2+}-doped Ultralong Hydroxyapatite Nanowires and Black Phosphorus Nanosheets for Accelerated Healing of Infected Wound [J]. *Chem Eng J*, 2022, **437**: 135347. DOI: 10.1016/j.cej.2022.135347.

[28] YU L, HE T T, YAO J, *et al*. Cu Ions and Cetyltrimethylammonium Bromide Loaded into Montmorillonite: a Synergistic Antibacterial System for Bone Scaffolds[J]. *Mater Chem Front*, 2022, **6**(1): 103−116. DOI: 10.1039/d1qm01278a.

[29] LI P, DING Z, YIN Y, *et al*. Cu^{2+}-doping of Polyanionic Brushes: a Facile Route to Prepare Implant Coatings with both Antifouling and Antibacterial Properties[J]. *Eur Polym J*, 2020, **134**: 109845. DOI: 10.1016/j.eurpolymj.2020.109845.